

# The Cyanobacterial “Nutraceutical” Phycocyanobilin Inhibits Cysteine Protease Legumain

Isabel V. L. Wilkinson,<sup>[a]</sup> Gabriel Castro-Falcón,<sup>[b]</sup> Maria C. Roda-Serrat,<sup>[c]</sup> Trevor N. Purdy,<sup>[b]</sup> Jan Straetener,<sup>[d]</sup> Melanie M. Brauny,<sup>[e, f]</sup> Lisa Maier,<sup>[e, f]</sup> Heike Brötz-Oesterhelt,<sup>[d, e, g]</sup> Lars P. Christensen,<sup>[c, h]</sup> Stephan A. Sieber,<sup>\*[a]</sup> and Chambers C. Hughes<sup>\*[b, d, e, g]</sup>

The blue biliprotein phycocyanin, produced by photo-autotrophic cyanobacteria including spirulina (*Arthrospira*) and marketed as a natural food supplement or “nutraceutical,” is reported to have anti-inflammatory, antioxidant, immunomodulatory, and anticancer activity. These diverse biological activities have been specifically attributed to the phycocyanin chromophore, phycocyanobilin (PCB). However, the mechanism of action of PCB and the molecular targets responsible for the beneficial properties of PCB are not well understood. We have developed a procedure to rapidly cleave the PCB pigment from

phycocyanin by ethanolysis and then characterized it as an electrophilic natural product that interacts covalently with thiol nucleophiles but lacks any appreciable cytotoxicity or antibacterial activity against common pathogens and gut microbes. We then designed alkyne-bearing PCB probes for use in chemical proteomics target deconvolution studies. Target identification and validation revealed the cysteine protease legumain (also known as asparaginyl endopeptidase, AEP) to be a target of PCB. Inhibition of this target may account for PCB’s diverse reported biological activities.


## Introduction


Phycocyanin is one of several photosynthetic proteins (“phycobiliproteins”) found in cyanobacteria, red algae, and cryptonoms. The deep blue color of phycocyanin originates from the bile pigment chromophore phycocyanobilin (PCB, 1), a highly conjugated linear tetrapyrrole that is covalently bound via a thioether linkage to a cysteine residue and serves as the primary light-absorbing material in light-harvesting phycobilisomes (Figure 1). Phycocyanobilin (2), phycobiliviolin (3), and phycocourobilin (4) are related phycobilins that serve a function similar to PCB in other phycobiliproteins.

Phycocyanin exhibits a wide range of beneficial biological activities stemming from its antioxidant, anti-inflammatory, and anticancer properties, in addition to various hepato-, nephro-, and cardioprotective properties.<sup>[1–4]</sup> Some studies have reported that phycocyanin has antibacterial activity against drug-resistant bacteria.<sup>[5]</sup> The recognized nutritional and health benefits of phycocyanin have led to the development of food supplements composed of *Arthrospira platensis* (“spirulina”), free-floating, filamentous cyanobacteria that are grown on an industrial scale in open raceway ponds. Many of the biological effects of phycocyanin have been attributed to the presence of PCB,<sup>[6]</sup> as the pigment itself is reported to have antioxidant,<sup>[7–9]</sup> anti-inflammatory,<sup>[10,11]</sup> anticancer,<sup>[12]</sup> and immunomodulatory

- [a] Dr. I. V. L. Wilkinson, Prof. Dr. S. A. Sieber  
Center for Protein Assemblies (CPA)  
Department of Chemistry, Technical University of Munich  
Ernst-Otto-Fischer-Str. 8, 85748, Garching (Germany)  
E-mail: stephan.sieber@tum.de
- [b] Dr. G. Castro-Falcón, Dr. T. N. Purdy, Dr. C. C. Hughes  
Center for Marine Biotechnology and Biomedicine  
Scripps Institution of Oceanography  
University of California  
San Diego, CA 92093 (USA)
- [c] Dr. M. C. Roda-Serrat, Prof. Dr. L. P. Christensen  
Department of Green Technology  
University of Southern Denmark  
Campusvej 55, 5230 Odense M (Denmark)
- [d] J. Straetener, Prof. Dr. H. Brötz-Oesterhelt, Dr. C. C. Hughes  
Department of Microbial Bioactive Compounds  
Interfaculty Institute of Microbiology and Infection Medicine  
University of Tübingen  
72076 Tübingen (Germany)  
E-mail: chambers.hughes@uni-tuebingen.de
- [e] M. M. Brauny, Prof. Dr. L. Maier, Prof. Dr. H. Brötz-Oesterhelt,

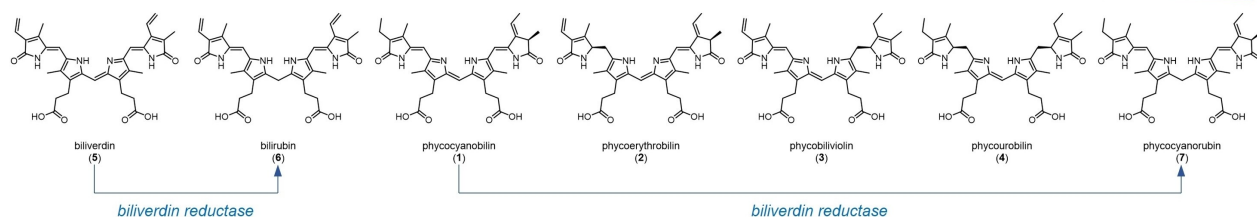
- Dr. C. C. Hughes  
Cluster of Excellence EXC 2124:  
Controlling Microbes to Fight Infection  
University of Tübingen  
72076 Tübingen (Germany)
- [f] M. M. Brauny, Prof. Dr. L. Maier  
Microbiome-Host-Interaction Lab  
Interfaculty Institute of Microbiology and Infection Medicine  
University of Tübingen  
72076 Tübingen (Germany)
- [g] Prof. Dr. H. Brötz-Oesterhelt, Dr. C. C. Hughes  
German Center for Infection Research  
Partner Site Tübingen  
72076 Tübingen (Germany)
- [h] Prof. Dr. L. P. Christensen  
Department of Physics, Chemistry and Pharmacy  
University of Southern Denmark  
Campusvej 55, 5230 Odense M (Denmark)

 Supporting information for this article is available on the WWW under <https://doi.org/10.1002/cbic.202200455>

 © 2022 The Authors. ChemBioChem published by Wiley-VCH GmbH. This is an open access article under the terms of the Creative Commons Attribution Non-Commercial License, which permits use, distribution and reproduction in any medium, provided the original work is properly cited and is not used for commercial purposes.

## A OXIDIZED

## REDUCED



## B

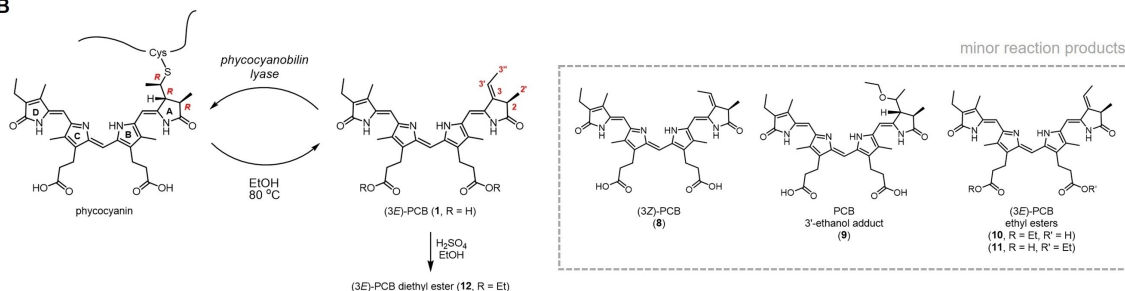


**Figure 1.** A) Structures of phycocyanobilin (1); related phycobilins phycoerythrobilin (2), phycobiliviolin (3), and phycocourobilin (4); heme catabolites biliverdin (5) and bilirubin (6); and phycocyanorubin (7). Biliverdin reductase, which reduces 5 to 6 in the liver as part of heme catabolism, also reduces 1 to 7, a structural analogue of 6. The bile pigments are arranged to show their level of oxidation. B) (3E)-Phycocyanobilin [(3E)-1] is liberated from phycocyanin using hot ethanol. (3Z)-PCB (8), PCB 3'-ethanol adduct 9, and (3E)-PCB ethyl esters 10 and 11 are also formed during this process. In the reverse, biosynthetic direction, 1 is attached to the phycocyanin apoprotein by phycocyanobilin lyase. (3E)-PCB diethyl ester 12 is formed by treatment of 1 with acidic ethanol.

properties<sup>[13,14]</sup> (recently reviewed<sup>[15]</sup>). Other linear tetrapyrroles such as biliverdin (5) and bilirubin (6) have been shown to have antioxidant and anti-mutagenic effects similar to 1, but these bile pigments are found in vertebrates in very small quantities, making them unsuitable for large-scale production.<sup>[8,16]</sup> To address this shortcoming, recombinant methods for the production of biliverdin (5) in *Escherichia coli* are being developed.<sup>[17]</sup>

The structure of 1 was first established using a combination of infrared, ultraviolet/visible, and nuclear magnetic resonance spectroscopy, as well as mass spectrometry in the late 1960s.<sup>[18,19]</sup> The discovery that the chromophore could be cleaved from the protein using refluxing methanol or strongly acidic conditions paved the way for the elucidation of the PCB structure. However, this elimination process also precluded investigations concerning the nature of the PCB-protein linkage. Unambiguous evidence that PCB was linked to C-phycocyanin via a cysteine thioether was obtained after it was discovered that treatment of the phycobiliprotein with cyanogen bromide gave a peptide-bound PCB fragment that could be examined by NMR spectroscopy.<sup>[20]</sup> The stereochemistry of cysteine-linked PCB was then determined to be 2*R*, 3*R*, 3'*R*.<sup>[21–24]</sup>

Previous studies have shown that PCB can be cleaved from the apoprotein by several methods including acid hydrolysis, enzymatic cleavage, and solvolysis in methanol.<sup>[18,19,25,26]</sup> In another example, treatment of *A. platensis* at pH 12 and sonication with glass pearls to prevent precipitation of phycocyanin delivered high yields of PCB.<sup>[27]</sup> We recently disclosed the finding that ethanolysis of a spirulina-based food colorant, LinaBlue, also produced PCB in high yield.<sup>[28]</sup> Using this

commercial source of phycocyanin resolved complications associated with collecting the organism and sufficiently degrading the cyanobacterial cell wall. Due to the striking panacea-like properties of PCB, the development of robust methods to produce PCB from phycocyanin continue to be reported.<sup>[29]</sup>

In this work, we characterized all of the reaction products that could be detected from the ethanolysis reaction using a variety of analytical and spectroscopic methods. In this way, we identified the principal product (3E)-PCB, as well as (3Z)-PCB, a PCB-ethanol adduct, and an inseparable mixture of PCB monoethyl esters present in minor amounts. We further characterized PCB as an electrophilic natural product that interacts covalently with thiol nucleophiles. We then designed alkyne-bearing PCB probes to deconvolute its molecular targets by chemical proteomics and thereby identified and validated PCB as an inhibitor of the cysteine protease legumain ( $IC_{50}$  of  $65 \pm 8 \mu\text{M}$ ).

## Results and Discussion

### Isolation and characterization of phycocyanobilin and congeners

In an effort to uncover the molecular basis for the reported biological properties of phycocyanin and PCB (1), we first sought to establish a reliable and facile method for the multi-milligram production of the pigment. Treatment of the food colorant with hot ethanol overnight liberated PCB (1) from phycocyanin, as indicated by the dark blue color of the resulting solution. PCB, however, was not the only product

formed, and so we meticulously purified and characterized all PCB-related side-products using liquid chromatography/high-resolution electrospray ionization quadrupole time-of-flight MS/MS (HPLC–ESI–QTOF–MS/MS) and NMR spectroscopy. The major product eluting at  $t_R = 10.9$  min was assigned as (3E)-PCB (1) on the basis of its UV/vis absorption spectrum ( $\lambda_{max} = 369, 659$  nm) and a pseudomolecular ion  $m/z$  587.2861  $[M+H]^+$  (calcd for  $C_{33}H_{39}N_4O_6$ , 587.2864; Figure 1 and Figures S1–S3 in the Supporting Information). Using a combination of  $^1H$ - $^1H$  COSY, HSQC, and HMBC NMR experiments, we were able to assign proton and carbon chemical shifts to every position (Table S1 and Figures S4–S7). A minor isomeric compound eluting at  $t_R = 11.9$  min was assigned as (3Z)-PCB (8), likewise on the basis of its UV/vis absorption spectrum ( $\lambda_{max} = 362, 640$  nm) and a pseudomolecular ion  $m/z$  587.2853  $[M+H]^+$  (calcd for  $C_{33}H_{39}N_4O_6$ , 587.2864). Comparison of the  $^1H$  NMR spectra for 1 and (3Z)-PCB (8) indicated a difference in the C-3/C-3' olefin configuration between the two stereoisomers (Table S2). Chemical shifts for  $H_{1-2'}$  ( $\delta_{H(1)} = 1.52$ ;  $\delta_{H(8)} = 1.45$ ),  $H_{1-3'}$  ( $\delta_{H(1)} = 6.34$ ;  $\delta_{H(8)} = 5.82$ ), and  $H_{3-3''}$  ( $\delta_{H(1)} = 1.72$ ;  $\delta_{H(8)} = 1.98$ ) differ significantly while all other proton signals were preserved between the two molecules (Table S2 and Figures S8–S11).

A third compound, eluting between (3E)-PCB (1) and (3Z)-PCB (8) at  $t_R = 11.2$  min, showed a hypsochromic shift in its UV/vis spectrum ( $\lambda_{max} = 347, 626$  nm) compared to PCB and analyzed for the molecular formula  $C_{35}H_{44}N_4O_7$  ( $m/z$  633.3293  $[M+H]^+$ , calcd for  $C_{35}H_{45}N_4O_7$ , 633.3283; Table S3 and Figures S12–S15). This 46 amu increase in mass was attributed to the addition of a molecule of ethanol. The COSY spin system from  $H_{1-3}$  [ $\delta_H = 3.22$  (overlapped);  $\delta_C = 51.8$ ] to  $H_{1-3'}$  [ $\delta_H = 4.00$  ( $t, J = 6.3$  Hz);  $\delta_C = 77.5$ ] to  $H_{3-3''}$  [ $\delta_H = 1.34$  ( $d, J = 6.2$  Hz);  $\delta_C = 16.8$ ] and relevant HMBC correlations from  $H_{3-3''}$  to C-3 and C-3' and from  $H_{3-2'}$  [ $\delta_H = 1.47$  ( $t, J = 7.3$  Hz)] to C-3 revealed the structure

of (3E)-PCB 3'-ethanol adduct (9; Table S3). The configuration at C-3' was not strictly determined.

Lastly, a 2:1 mixture of (3E)-PCB mono-ethyl esters (10/11), co-eluting at  $t_R = 13.4$  min, each analyzed for the molecular formula with  $C_{35}H_{42}N_4O_6$  ( $m/z$  615.3176  $[M+H]^+$ , calcd for  $C_{35}H_{43}N_4O_6$ , 615.3177; Tables S4 and S5, Figures S16–S19). The structure of the major isomer was deduced from key HMBC correlations from the ethyl ester methylene protons ( $H_{2-20}$ ,  $\delta_H = 4.14$ ;  $\delta_C = 60.8$ ) to the C-8''' or C-12''' carbonyl carbon ( $\delta_C = 173.2$ ; Tables S4 and S5). Methylene proton signals ( $H_{2-20}$ ,  $\delta_H = 4.14$ ;  $\delta_C = 60.8$ ) corresponding to the ethyl ester in the minor isomer overlap with those from the major isomer but are still distinguishable. Presumably, these PCB derivatives are formed by acid-catalyzed esterification. In line with this observation, the deliberate treatment of 1 with sulfuric acid in ethanol at room temperature furnished (3E)-PCB diethyl ester (12; Figures S20 and S21).

### Antibacterial activity and cytotoxicity of phycocyanobilin

Given this facile route to the pure PCB (1), we set out to thoroughly assess its biological activity in vitro towards a variety of pathogens and three human cancer cell lines (Figure 2). Both (3E)-PCB (1) and (3E)-PCB diethyl ester (12) showed MICs of  $> 64 \mu\text{g mL}^{-1}$  against all ESKAPE pathogen species as well as *Bacillus subtilis* 168 and *E. coli* ATCC25922. (3E)-PCB (1) also showed MICs of  $> 64 \mu\text{g mL}^{-1}$  against members of the human gut microbiome, including *Bacteroides vulgatus* ATCC8482, *Roseburia intestinalis* CIP107878, and *Fusobacterium nucleatum* ATCC25586. This lack of activity against bacteria is favorable, as the compounds are not likely to disrupt the homeostasis of the gut microbiome. Furthermore, 1 and 12 showed no appreciable

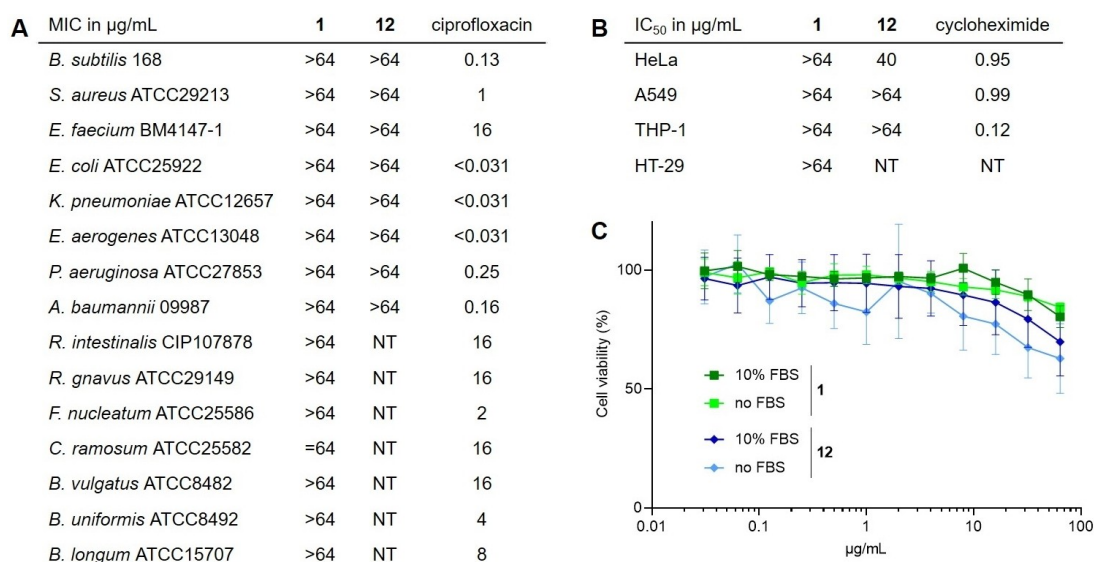


**Figure 2.** A) Minimal inhibitory concentrations (MIC) of (3E)-PCB (1) and (3E)-PCB diethyl ester (12) against *B. subtilis* 168, *E. coli* ATCC25922, ESKAPE pathogens, and seven representative bacterial species of the human gut microbiome. B) Half maximal inhibitory concentrations (IC<sub>50</sub>) of 1 and 12 against epithelial cervix adenocarcinoma HeLa, lung adenocarcinoma A549, monocytic THP-1, and human colon adenocarcinoma HT-29 cell lines. C) Comparison of the IC<sub>50</sub> of 1 and 12 against A549 in cell culture medium supplemented with 10% fetal bovine serum (FBS) versus culture medium without FBS.

cytotoxicity against HeLa cells ( $IC_{50} > 64 \mu\text{g mL}^{-1}$  and  $40 \mu\text{g mL}^{-1}$ , respectively) and no cytotoxicity against A549 cells and THP-1 cells in the tested range ( $IC_{50} > 64 \mu\text{g mL}^{-1}$ ). Against intestinal cell line HT-29, PCB 1 also displayed no cytotoxicity. To exclude a putative inhibitory effect of albumin contained in the fetal calf serum additive to the cell culture medium, which could potentially mask the detection of cytotoxic effects by binding to PCP and reducing its free fraction,<sup>[30]</sup> we repeated our cytotoxicity assay for **1** and **12** and the A549 cell line in serum-free medium. Cytotoxicity was not enhanced. This lack of antibacterial activity and cytotoxicity for **1** is surprising considering the electrophilic nature of PCB (see below) but reassuring given the widespread use of phycocyanin as a food colorant and dietary supplement. Although the results of these cell-killing assays are significant, they are not likely to reflect the beneficial biological properties purported for phycocyanin and, by inference, **1**.

### Thiol reactivity of phycocyanobilin

In line with our previous efforts to identify naturally occurring covalent inhibitors or “electrophilic natural products” by chemical labeling with readily detectable thiol probes, PCB **1** was shown to react with 4-bromothiophenol (**13**) in dimethylformamide ( $m/z$  775.2132 [ $M+H$ ]<sup>+</sup>, calcd for  $C_{39}H_{44}BrN_4O_6S$ , 775.2159; Figures 3, S22 and S23).<sup>[31]</sup> The exact structure of the PCB thiol adduct (**14**) was determined by NMR spectroscopy, which confirmed the site of thiol addition at C-3' of PCB (Table S6, Figures S24–S27). COSY spin systems and HMBC correlations analogous to those for the PCB 3'-ethanol adduct (**9**) were observed, with one key difference being that the carbon chemical shift at C-3' was much lower ( $\delta_C = 48.2$ ), as expected. Reaction of **13** with semisynthetic PCB diester **12** gave an analogous product (**15**; Table S7, Figures S28–S33). The overall process mimics the biosynthetic reaction for attachment of PCB to the phycocyanin apoprotein (Figure 1).

### Cellular target of phycocyanobilin

We therefore sought to exploit the electrophilic nature of PCB to elucidate its protein binding partners through affinity

capture.<sup>[32,33]</sup> A chemical proteomics approach to target identification was thus envisioned using PCB-based probes bearing a click handle for subsequent ligation to a detection or enrichment handle (e.g., a fluorophore or biotin) to enable identification of protein binding partners by LC–MS/MS analysis (Figure 4A).<sup>[34–38]</sup> The commonly used alkyne tag was chosen for its small size as the click handle and the carboxylic acid groups of PCB were chosen as the sites for functionalization (Figure 4B).<sup>[39]</sup> Monoamide PCB probe **16** (isolated as a mixture of inseparable regioisomers) and diamide probe **17** were synthesized under standard coupling conditions with propargylamine and HATU (Figures S34–S37). The design of the probes (without a photoaffinity group<sup>[40]</sup>) was intended for the discovery of targets interacting covalently with PCB.

In order to assess the capacity for protein binding, live HEK293 cells were treated with the probes in a range of concentrations (0.1–10  $\mu\text{M}$ , 1% DMSO *v/v*) for 2 h (37 °C) in serum-free media. The serum was excluded to improve the availability of the probe in solution as PCB is known to bind bovine serum albumin with an affinity of  $2 \times 10^6 \text{ M}^{-1}$ .<sup>[41]</sup> After cell lysis and click reaction to TAMRA-azide, probe-treated lysates were subjected to SDS-PAGE. Fluorescent imaging revealed dose-dependent labeling of proteins and no labeling in the DMSO-only vehicle control (Figure 4C).

We next proceeded to target identification by chemical proteomics using the lowest probe concentration where protein labeling was observed (1  $\mu\text{M}$  treatment) to help minimize non-specific binding. After click-mediated ligation of probe-labeled proteins to biotin-azide, affinity enrichment with avidin beads under denaturing conditions (6 M urea) and on-bead tryptic digest, the resulting peptides were analyzed by quantitative LC–MS/MS. Determination of proteins significantly enriched by probes **16** and **17** was performed using an empirical Bayes approach implementing<sup>[42]</sup> the R Bioconductor package *limma*<sup>[43]</sup> in order to increase the power of the statistical inference compared to ordinary two-sample *t*-tests by estimating sample variance based not only on the data obtained for each protein alone but also the global variability across the whole dataset (Figures 4D and S39, list of proteins in supplementary dataset, raw data available in the PRIDE repository<sup>[44]</sup>).<sup>[45]</sup>

Legumain (LGMN, also known as asparaginyl endopeptidase, AEP) was statistically and significantly enriched by both probes ( $p < 0.05$  for probe **16**,  $p < 0.0005$  for probe **17**, Fig-

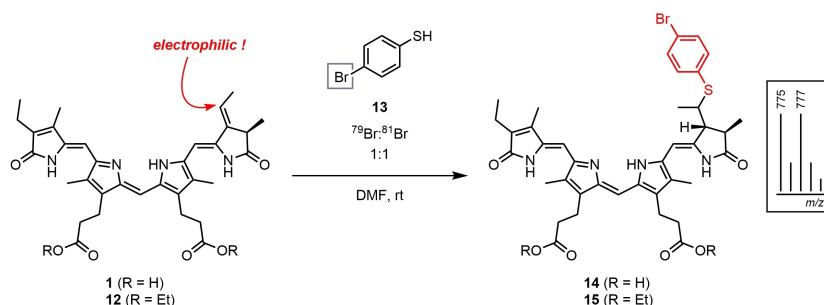


**Figure 3.** Treatment of **1** and **12** with thiophenol **13**, a probe for electrophilic natural products, yielded PCB thiol adducts **14** and **15**, respectively.



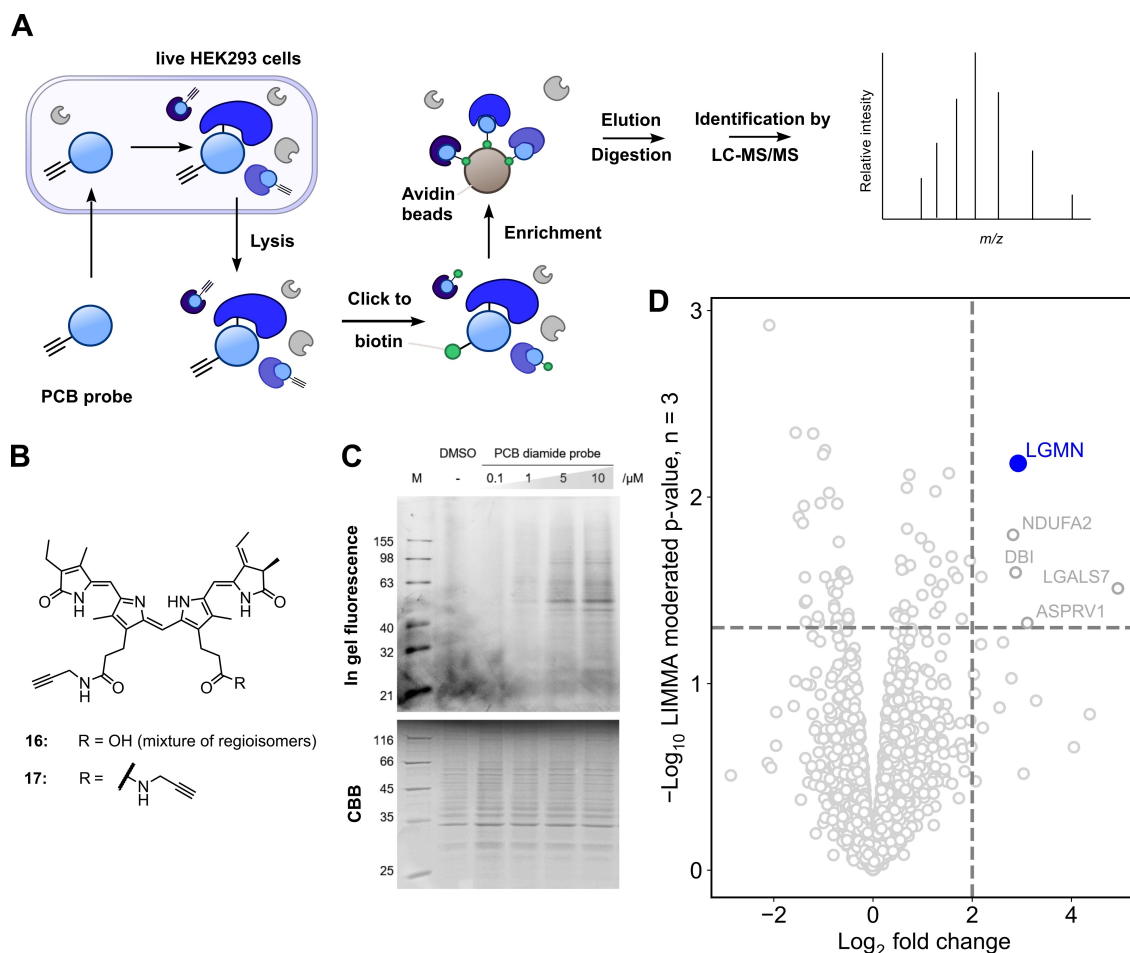


**Figure 4.** A) Schematic for the chemical proteomics approach used to identify the protein targets of PCB. HEK293 cells were treated (2 h, 37 °C) with alkyne-bearing monoamide PCB probe **16** (mixture of regioisomers) or diamide **17** (each 1  $\mu\text{M}$ ) or DMSO (vehicle control, 1% v/v). Following cell lysis, a copper-catalyzed click reaction to biotin-azide was performed, and biotinylated samples were enriched on avidin beads. After tryptic digestion, peptides were analyzed by liquid chromatography-tandem mass spectrometry (LC-MS/MS). B) Structures of PCB-derived probes **16** and **17**. C) TAMRA-treated samples were separated by SDS-PAGE, and labeled proteins were visualized by in-gel fluorescence. Total protein content was visualized using Coomassie Brilliant Blue (CBB) as a loading control. Uncropped gel images can be found in Figure S38. D) Volcano plot of proteins enriched using probe **17**. Fold change and significance of protein enrichment upon probe treatment vs. DMSO control were calculated by using a LIMMA-moderated t-test (implemented in R). The cysteine protease legumain (LGMN) was identified as the top hit for probe **17**. TAMRA: tetramethylrhodamine, SDS-PAGE: sodium dodecyl sulfate-polyacrylamide gel electrophoresis, LIMMA: linear model to microarray data.

ure S39) and was consequently advanced to target validation studies. First, binding of the PCB probe **17** (20  $\mu\text{M}$ ) to recombinant prolegumain enzyme (1  $\mu\text{M}$ ) spiked into HEK293 lysate (2-h incubation, 37 °C) was investigated. Following click reaction to TAMRA-azide, the appearance of a fluorescent band in the SDS-PAGE (denaturing) gel corresponding to legumain indicated covalent binding of the probe to the protein (Figure S40). Next, the binding of unmodified PCB to legumain was investigated by co-treatment of PCB and PCB probe **17** on the spiked-in lysate. In the presence of excess PCB, the fluorescent labeling of the enzyme by the PCB probe was no longer observed (Figure 5A), indicating binding of PCB to legumain in a manner competitive to the PCB probe.

Legumain is conserved across mammals, plants and invertebrate parasites and has multifarious physiological and pathological roles, including endopeptidase, carboxypeptidase,<sup>[46]</sup> ligase<sup>[47]</sup> and even transcription factor<sup>[48]</sup> activities, depending

on context (localization, pH, redox potential, cofactor, substrate etc.).<sup>[49,50]</sup> Its proteolytic activity is involved in antigen presentation to the MHC II complex<sup>[51]</sup> and immune signaling<sup>[52–54]</sup> making it a downstream modulator of the immune response. In addition, legumain is overexpressed in many types of solid tumors, including breast, colon, lung, prostate and ovarian cancer, and is believed to participate in regulation of tumor angiogenesis and invasion.<sup>[55]</sup> High legumain activity correlates with enhanced cancer growth and metastasis, as well as a poor patient prognosis.<sup>[56–60]</sup> Given the key roles of legumain in immunity and cancer, inhibition of its activity could therefore potentially match the PCB treatment phenotype.

The ability of PCB to inhibit the endopeptidase activity of legumain was therefore investigated in an in vitro assay using an activated recombinant enzyme and the synthetic fluorogenic substrate Z-Ala-Ala-Asn-AMC.<sup>[61]</sup> Here, PCB was found to

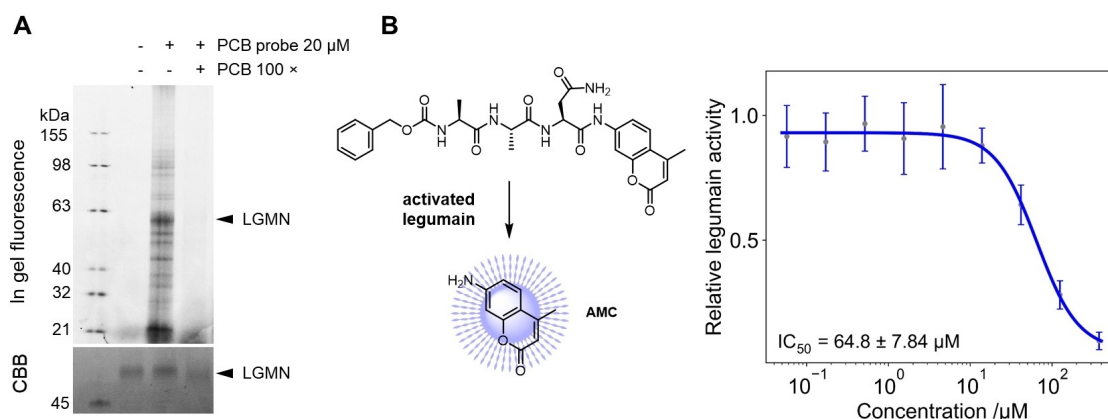


**Figure 5.** Validation of legumain as a target of PCB. A) Fluorescent labeling of recombinant prolegumain (1  $\mu\text{M}$  spiked into 5  $\mu\text{g}$  HEK293 lysate) by PCB probe 17 (20  $\mu\text{M}$ ) is outcompeted in the presence of a 100-fold excess of the parent compound PCB. Error bars represent the standard deviation of four replicates. B) The asparaginyl endopeptidase activity of legumain is inhibited by PCB. LGMN: legumain, AMC: 7-amino-4-methylcoumarin, CBB: Coomassie Brilliant Blue,  $\text{IC}_{50}$ : half maximal inhibitory concentration, PCB: phycocyanobilin.

inhibit legumain with a calculated  $\text{IC}_{50}$  of  $65 \pm 8 \mu\text{M}$ , thus confirming it as a molecular target of the natural product.

## Conclusion

Phycocyanobilin is a natural product with a range of intriguing properties including antioxidant, anti-inflammatory, anticancer, and immunomodulatory activities. Herein, we have reported a rapid method for its isolation on a multi-milligram scale from a commercial spirulina-based food colorant. We then tested it against a panel of bacterial pathogens, gut microbes, and human cancer cell lines, thereby demonstrating a favorable lack of activity against prokaryotic and eukaryotic cells. We further designed and synthesized two alkyne-bearing probes in order to rationalize PCB's mechanism of action and elucidated its molecular target in live human cells. Analysis of probe-bound proteins using quantitative mass spectrometry identified legumain (LGMN, asparaginyl endopeptidase, AEP) as the top hit. A total of 3193 proteins were identified in our proteomics experiments. Aside from LGMN, only a handful of proteins were significantly enriched by the PCB probes; this suggests a small number of protein (off)-targets and underscores PCB's good safety profile.<sup>[62]</sup> However, we cannot exclude the presence of other protein targets not detected in our proteomics experiments that might contribute to PCB's reported activities.

In validation studies, PCB was found to bind legumain, competitively displacing its probe derivative, and further found to inhibit legumain endopeptidase activity with an  $\text{IC}_{50}$  of  $65 \pm 8 \mu\text{M}$ . While there are many other and more potent legumain inhibitors already reported in the literature<sup>[63–69]</sup> (and recently reviewed<sup>[70]</sup>), this is the first report of PCB as a legumain inhibitor. The fact that PCB is an orally bioavailable component of a safe and well-tolerated food supplement distinguishes it from existing legumain inhibitors, which are typically chemical probes with poor pharmacokinetic properties. The discovery of

PCB's inhibition of legumain might account for its diverse reported biological activities.

## Experimental Section

**General experimental:** The phycocyanin-based colorant Linablu G1 was purchased from DIC Europe GmbH (Düsseldorf, Germany). All other reagents and solvents were purchased commercially and were used without further purification. Reaction mixtures were analyzed on an analytical 1100 Series Agilent Technologies HPLC system coupled to UV/vis (210, 254, and 360 nm) and evaporative light-scattering detector (ELSD) using a Phenomenex Luna reversed-phase C18(2) column (100  $\times$  4.6 mm, 5  $\mu\text{m}$ , 100  $\text{\AA}$ ) with a 10 or 20 gradient from 10–100%  $\text{CH}_3\text{CN}$  in water containing 0.1% formic acid and a 1.0 or 0.7  $\text{mL min}^{-1}$  flow rate. Using the same column and a 20 min gradient from 10–100%  $\text{CH}_3\text{CN}$  in water containing 0.1% formic acid and a 0.7  $\text{mL min}^{-1}$  flow rate, HPLC-ESI-QTOF-MS/MS was performed on an analytical Agilent 1260 Infinity Series LC system coupled to a 6530 Series QTOF mass spectrometer. Column chromatography was performed on a Teledyne CombiFlash Rf + Lumen flash chromatography system. Preparative reversed-phase HPLC was performed using a Millipore Waters 600E solvent delivery system with a Phenomenex Luna C18(2) column (250  $\times$  21.2 mm, 5  $\mu\text{m}$ , 100  $\text{\AA}$ ) and a 13  $\text{mL min}^{-1}$  flow rate or a Phenomenex Luna silica column (250  $\times$  21.2 mm or 250  $\times$  10 mm, 5  $\mu\text{m}$ , 100  $\text{\AA}$ ) and a 13 or 3  $\text{mL min}^{-1}$  flow rate. Compounds were detected with a single-wavelength Knauer UV detector at 254 nm or 360 nm.  $^1\text{H}$  NMR spectra at 500 MHz or 400 MHz on a Jeol 500 MHz or Bruker Avance III HDX 400 MHz spectrometer in  $[\text{D}_5]\text{pyridine}$  (residual solvent referenced to 7.22 ppm).

**Ethanolysis reaction:** A suspension of Linablu G1 (20 g) in 96% ethanol (250 mL) in a 500 mL round-bottomed flask was heated under reflux overnight in an oil bath at 95  $^\circ\text{C}$ . The solution was allowed to cool and then directly filtered through a fritted Büchner funnel to remove precipitated protein. The deep blue filtrate was concentrated to yield 1.4 g of crude material. Before HPLC purification, one of two methods was used to remove sugars and other hydrophilic byproducts. Method A: The crude material was fractionated on a flash chromatography system (4 g C18 cartridge, 360 nm) with a 15 min solvent gradient from 10–100% solvent B (solvent A: water with 5 mM ammonium formate, pH 3.2; solvent B:

9:1 methanol/water with 5 mM ammonium formate, pH 3.2) and a 18 mL min<sup>-1</sup> flow rate. Fractions containing PCB and derivatives were combined in separate flasks and concentrated to dryness. Method B: The crude material was diluted with water (1 L) and extracted with EtOAc (3 × 200 mL). The combined extracts were washed with brine (100 mL), dried over sodium sulfate, and concentrated to dryness to give 30 mg of crude PCB.

**Purification of PCB (1) and PCB derivatives (8, 9, 10/11):** The solvolysis reaction products were purified using reversed-phase HPLC (Millipore Waters 600E) with a Phenomenex Luna C18(2) preparative column (250 × 21.2 mm, 5 μm, 100 Å) using isocratic conditions with 80% solvent B (solvent A: water with 5 mM ammonium formate, pH 3.2; solvent B: 9:1 methanol/water with 5 mM ammonium formate, pH 3.2) and a 13 mL min<sup>-1</sup> flow rate. The fractions containing pure 1, 8, 9, and 10/11 were combined in separate flasks, methanol was removed from each solution with a rotary evaporator, and the remaining aqueous solutions were frozen and lyophilized. The compounds were characterized by <sup>1</sup>H and 2D NMR spectroscopy, UV/vis spectroscopy, and high resolution mass spectrometry (see the Supporting Information).

**PCB diethyl ester (12):** To a solution of crude PCB (20 mg) at room temperature was added a 50:1 EtOH/H<sub>2</sub>SO<sub>4</sub> solution (2 mL). After 12 h at room temperature, the mixture was diluted with EtOAc (25 mL), washed successively with water (25 mL) and brine (25 mL), dried over sodium sulfate, and concentrated to give 20 mg of crude PCB diethyl ester. The product was purified by preparative normal-phase HPLC with 2% solvent B (solvent A: DCM; solvent B: MeOH) to give diester 12. The compound was characterized by <sup>1</sup>H NMR spectroscopy and high resolution mass spectrometry (see the Supporting Information).

**PCB thiophenol adduct (14):** To a solution of crude PCB (10 mg) in *N,N*-dimethylformamide (1 mL) at room temperature under nitrogen atmosphere was added 4-bromothiophenol (13; 5.0 mg, 0.026 mmol). After 12 h at room temperature, the mixture was analyzed by HPLC as described above. The product was purified by preparative reversed-phase HPLC with 55% solvent B (solvent A: water with 0.1% formic acid; solvent B: acetonitrile with 0.1% formic acid) to give 4.0 mg of thiol adduct 14. The compound was characterized by <sup>1</sup>H and 2D NMR spectroscopy, UV/vis spectroscopy, and high resolution mass spectrometry (see the Supporting Information).

**PCB diethyl ester thiophenol adduct (15):** To a solution of crude PCB diethyl ester (10 mg) in *N,N*-dimethylformamide (1 mL) at room temperature under nitrogen atmosphere was added 4-bromothiophenol (13; 5.0 mg, 0.026 mmol). After 12 h at room temperature, the mixture was analyzed by HPLC as described above. The product was purified by preparative normal-phase HPLC with 35% solvent B (solvent A: hexane; solvent B: ethyl acetate) to give 1.4 mg of thiol adduct 15. The compound was characterized by <sup>1</sup>H and 2D NMR spectroscopy, UV/vis spectroscopy, and high resolution mass spectrometry (see the Supporting Information).

**PCB monoamide (16) and diamide (17):** To a solution of crude PCB (30 mg) and HATU (15 mg, 0.039 mmol) in DMF (1 mL) at room temperature under nitrogen atmosphere was added Et<sub>3</sub>N (20 μL, 0.14 mmol) and propargylamine (20 μL, 0.31 mmol). After 1 h the mixture was analyzed by HPLC as described above, then diluted with DCM (100 mL) and brine (100 mL). The DCM layer was dried, filtered, and concentrated to 40 mL. The solution was injected from a syringe onto a 12 g silica cartridge preconditioned with DCM, and the products were purified on a flash chromatography system (12 g silica cartridge, 254 nm) with a 12 min solvent gradient from 0–20% solvent B (solvent A: DCM; solvent B: MeOH) and a 30 mL min<sup>-1</sup> flow rate to yield 4.9 mg of monoamide 16 (*t*<sub>R</sub> = 6–

6.5 min) and 5.5 mg of diamide 17 (*t*<sub>R</sub> = 7.5–9.5 min). The compounds were characterized by <sup>1</sup>H NMR spectroscopy and high resolution mass spectrometry (see the Supporting Information).

**Antimicrobial assays:** Antimicrobial activity against ESKAPE pathogens *B. subtilis* and *E. coli* was determined in accordance to the guidelines of the Clinical and Laboratory Standards Institute (CLSI).<sup>[71]</sup> Twofold dilutions of the test compounds starting from 64 μg mL<sup>-1</sup> were prepared in cation-adjusted Mueller–Hinton broth (BD Difco) in 96-well round bottom polystyrol plates (Sarstedt) with each well containing 50 μL of test compound solution at twice the final concentration. The wells were then inoculated with 50 μL of the bacterial suspension of the test strains at a final inoculum of 5 × 10<sup>5</sup> colony-forming units (CFU) mL<sup>-1</sup> in 100 μL final volume. The plates were incubated at 37 °C for 20 h, and the minimal inhibitory concentration (MIC) was determined as the lowest concentration of test compound that inhibited visible bacterial growth. In addition, MICs for seven bacterial species of the most prevalent and abundant phyla of the human gut microbiome were determined as described previously.<sup>[72]</sup> Species selection comprised *Bifidobacterium longum* ATCC15707 (Actinobacteria), *B. vulgatus* ATCC8482 (Bacteroidetes), *Bacteroides uniformis* ATCC8492 (Bacteroidetes), *Clostridium ramosum* ATCC25582 (Firmicutes), *R. intestinalis* CIP107878 (Firmicutes), *Ruminococcus gnavus* ATCC29149 (Firmicutes) and *F. nucleatum* (Fusobacteria) ATCC25586. Briefly, the strains were first grown overnight on BHI plates and then overnight in liquid mGAM media (Hyserve) under anaerobic conditions (Coy Laboratory Products Inc.). The cultures were diluted to an OD of 0.02, and aliquots (50 μL) were added to the wells of a 96-well round bottom plate with each well containing 50 μL of test compound solution at twice the final concentration. Bacterial growth was monitored for 22 h using hourly OD measurements in a BioTek Epoch 2 microplate reader under anaerobic conditions. The experiment was conducted in two independent biological replicates, and growth curves were analyzed as previously described using R.<sup>[72]</sup> MICs were defined as the lowest concentration for which the normalized AUC (area under the growth curve normalized to AUC of the untreated control) dropped below 0.2.

**Cytotoxicity assays:** Cytotoxicity evaluation was performed using a 7-hydroxy-3*H*-phenoxazin-3-one 10-oxide (resazurin) assay in RPMI cell culture medium (Gibco Life Technologies) supplemented with 10% heat-inactivated fetal bovine serum (Gibco Life Technologies) for the HeLa and THP-1 cell lines, Dulbecco's modified Eagle's medium (DMEM) cell culture medium (Gibco Life Technologies) supplemented with 10% heat-inactivated fetal bovine serum for the A549 cell line or Panserin 401 serum-free cell culture medium (Gibco Life Technologies) for the A549 cell line. A twofold serial dilution of the test compounds was prepared in a 96-well polystyrene microtiter plate and seeded with THP-1 or trypsinized HeLa or A549 cells to a final cell concentration of 1 × 10<sup>4</sup> cells per well. After 24 h of incubation at 37 °C, 5% CO<sub>2</sub>, and 95% relative humidity, resazurin was added to a final concentration of 200 μM, and cells were again incubated overnight. Cell viability was assessed by determining the reduction of resazurin to resorufin by measuring the fluorescence in a Tecan Infinite M200 Pro reader at an excitation wavelength of 560 nm and an emission wavelength of 600 nm in relation to an untreated control. HT-29 cells were grown in DMEM (Gibco Life Technologies) supplemented with 10% FBS and 1% penicillin/streptomycin at 37 °C, 12% CO<sub>2</sub>, and saturated humidity. For cytotoxicity testing, the Promega CellTiter 96<sup>®</sup> AQueous one solution cell proliferation assay was performed. In short, 2 × 10<sup>4</sup> cells per 100 μL were seeded into 72 wells of a flat bottom 96-well cell culture plate (Thermo Scientific), and the other 24 wells were filled with pure DMEM in order to serve as control wells for blank correction. Plates were incubated at 37 °C, 12% CO<sub>2</sub>, and saturated humidity for 24 h before the media was removed



and replaced with antibiotic-free DMEM due to the possible influence of antibiotics on the assay. The next day, PCB (1.5 mg) was mixed with 234  $\mu\text{L}$  DMSO to reach a PCB concentration of 6.4  $\text{mg mL}^{-1}$ , and a 2-fold serial dilution in DMSO down to 0.2  $\text{mg mL}^{-1}$  was performed. Each solution was once more diluted 1:100 in Hanks' balanced salt solution (HBSS, Thermo Fischer Scientific) to reach the final testing concentrations ranging from 2 to 64  $\mu\text{g mL}^{-1}$ . After removal of the antibiotic-free DMEM, 100  $\mu\text{L}$  of the PCB testing solutions were added to respective wells of the cell culture plate. Control columns containing 1% DMSO, 100% DMSO, and 100% HBSS were added, and cells were allowed to grow in the conditions described above. After 1.5 h, 20  $\mu\text{L}$  of the Promega CellTiter96<sup>®</sup> Aqueous one solution reagent was added into each of the filled wells, and the plate was again incubated for 1 h at 37 °C, 12% CO<sub>2</sub>, and saturated humidity. Cell viability was assessed by OD measurement to determine the presence of the produced formazan product indicating metabolically active and therefore living cells using a Tecan reader (490 nm, 5 s shaking, 3 mm). Bioinformatic analysis of the data was conducted with Excel and GraphPad Prism9.

**Cell culture for chemical proteomics:** Human embryonic kidney 293 (HEK293) cells were purchased from LGC Standards (ATCC-CRL-1573) and cultivated in a T175 culture flask (Sarstedt) containing high glucose DMEM (Sigma–Aldrich) supplemented with 10% heat-inactivated fetal bovine serum (FBS) (Sigma–Aldrich) and 2 mM L-glutamine (Sigma–Aldrich). Cells were maintained at 37 °C in a humidified 5% CO<sub>2</sub> atmosphere.

**Chemical proteomics workflow for labeling in HEK293 cells followed by SDS-PAGE:** 0.75 million HEK293 cells were seeded per well in poly-L-lysine-treated 6-well plates and grown to 90% confluency (~24 h, 37 °C, 5% CO<sub>2</sub>). The medium was then aspirated, the cells washed with PBS (2 × 1 mL), then incubated with serum-free media containing 1% DMSO (v/v) and various concentrations of PCB probe 16 or 17 (0–10  $\mu\text{M}$ ) for 2 h (37 °C, 5% CO<sub>2</sub>). After media removal and washing with PBS (2 × 1 mL), cells were lysed (4 °C, 10 min) with 200  $\mu\text{L}$  lysis buffer (1% NP40, 1% sodium deoxycholate, 0.1% sodium dodecyl sulfate, 1 × Roche cComplete™ EDTA-free mini protease inhibitor cocktail in PBS). Lysates were collected by scraping and sonicated (2 × 10 s pulses, 20% amplitude). The lysates were clarified (13 000 rpm, 4 °C, 15 min), and the protein concentration of the supernatant determined by BCA assay (Roti Quant, Roth). 75  $\mu\text{g}$  of lysate at 0.75  $\text{mg mL}^{-1}$  protein concentration per sample was subjected to a click reaction using 0.2 mM 5-TAMRA-azide (10 mM stock in DMSO, baseclick, BCFA-008), 1 mM TCEP (52 mM stock in ddH<sub>2</sub>O, Roth), 0.1 mM TBTA ligand (1.67 mM stock in 4:1 *t*-butanol/DMSO, TCI), and 1 mM CuSO<sub>4</sub> (50 mM stock in ddH<sub>2</sub>O) for 1 h (25 °C, 1000 rpm shaking). The reaction mixture was diluted with 50  $\mu\text{L}$  2 × SDS loading buffer (63 mM Tris·HCl, 10% glycerol, 139 mM SDS, 0.0025% bromophenol blue, 5% 2-mercaptoethanol), and the samples heated for 5 min at 95 °C. Each sample was mixed, and 40  $\mu\text{L}$  loaded per lane on an SDS-PAGE gel (12.5% acrylamide). A Fujifilm LAS 4000 luminescent image analyzer equipped with a Fujinon VRF43LMD3 lens and a 575DF20 filter (both Fujifilm) was used to fluorescently image the gel. Total protein content was monitored by staining with Coomassie Brilliant Blue.

**Chemical proteomics workflow for labeling in HEK293 cells followed by LC-MS/MS:** 3.5 million HEK293 cells were seeded in poly-L-lysine treated 10 cm dishes in triplicate and grown to 90% confluency (~24 h, 37 °C, 5% CO<sub>2</sub>). The medium was then aspirated, the cells washed with PBS (2 × 5 mL), then incubated with serum-free media containing 1% DMSO (v/v) and PCB probe 16 or 17 (1  $\mu\text{M}$ ) for 2 h (37 °C, 5% CO<sub>2</sub>). After media removal and washing with PBS (2 × 5 mL), cells were lysed (4 °C, 10 min) with 1 mL lysis buffer (1% NP40, 1% sodium deoxycholate, 0.1% SDS, 1 × Roche

cComplete™ EDTA-free mini protease inhibitor cocktail in PBS). Lysates were collected by scraping and sonicated (2 × 10 s pulses, 20% amplitude). The lysates were clarified (13 000 rpm, 4 °C, 15 min), and the protein concentration of the supernatant determined by BCA assay (Roti Quant, Roth). 600  $\mu\text{g}$  of lysate at 1.5  $\text{mg mL}^{-1}$  protein concentration per sample was subjected to a click reaction using 0.2 mM biotin-PEG<sub>3</sub>-azide (10 mM stock in DMSO, Sigma #762024), 1 mM TCEP (52 mM stock in ddH<sub>2</sub>O, Roth), 0.1 mM TBTA ligand (1.67 mM stock in 4:1 *t*-butanol/DMSO, TCI), and 1 mM CuSO<sub>4</sub> (50 mM stock in ddH<sub>2</sub>O) for 1 h (25 °C, 1000 rpm shaking). Excess click reagents were removed by protein precipitation using 4 volumes of acetone (−20 °C, 16 h), followed by washing of the protein pellet with MeOH (2 × 1 mL) with sonication (10% intensity, 10 s) to resuspend the pellet. The proteins were then solubilized with sonication in 500  $\mu\text{L}$  0.4% SDS in PBS. Avidin-agarose beads (Sigma, #A9207) were washed (3 × 1 mL 0.4% SDS in PBS), and 50  $\mu\text{L}$  added to each sample. After 1 h rotation (25 °C), the supernatant was removed, and the beads washed (3 × 1 mL 0.4% SDS in PBS, 3 × 1 mL 6 M urea in water, 3 × 1 mL PBS). The beads were resuspended in 200  $\mu\text{L}$  of 7 M urea, 2 M thiourea in 20 mM HEPES, pH 7.5, and on-bead proteins were reduced (5 mM TCEP, 1 h, 37 °C) and alkylated with iodoacetamide (final concentration 10 mM, 30 min, 25 °C). Alkylation was quenched with DTT (final concentration 10 mM, 30 min, 25 °C), and the proteins were then digested with LysC (0.5  $\mu\text{g}$ , Wako, 1 h, 25 °C). The samples were diluted with 600  $\mu\text{L}$  50 mM triethylammonium bicarbonate buffer and digested with trypsin (1.5  $\mu\text{g}$ , Promega, 15 h, 37 °C). Tryptic digest was terminated with the addition of 10  $\mu\text{L}$  formic acid (FA) and the trypsinized peptides were desalted with 50 mg Sep-Pak C18 cartridges (Waters Corp.). Desalted peptides were dried, then reconstituted in 40  $\mu\text{L}$  1% FA using a water bath sonicator and filtered through 0.22  $\mu\text{m}$  Ultrafree-MC centrifugal filters (Merck, UFC30GVNB). Samples were stored at −20 °C until LC-MS/MS measurement (1  $\mu\text{L}$  injection) on a Q Exactive Plus instrument (Thermo Fisher) coupled to an UltiMate 3000 nano-HPLC (Dionex) equipped with an Acclaim C18 PepMap100 75  $\mu\text{m}$  ID × 2 cm trap column (Thermo Fisher) and a 25 cm Aurora Series emitter column (25 cm × 75  $\mu\text{m}$  ID, 1.6  $\mu\text{m}$  FSC C18, Ionoptics) in an EASY-spray setting. Both columns were heated to 40 °C during the measurement process. Samples were first loaded on the trap column with 0.1% trifluoroacetic acid (TFA; 5  $\mu\text{L min}^{-1}$  flow rate), and then transferred to the separation column for a 152 min gradient using buffer A: H<sub>2</sub>O with 0.1% FA, buffer B: acetonitrile with 0.1% FA and 0.400  $\mu\text{L min}^{-1}$  flow rate. The gradient consisted of the following steps: buffer B at 5% for 7 min, gradient increase of buffer B to 22% over 105 min, then to 32% over the subsequent 10 min and finally to 90% over 10 min. 90% buffer B was then maintained for another 10 min before decreasing over 0.1 min to 5% for the rest of the run. Peptides were ionized at a capillary temperature of 275 °C, and the instrument was operated in a Top12 data dependent mode. For full scan acquisition, the Orbitrap mass analyzer was set to a resolution of  $R=140\,000$ , an automatic gain control (AGC) target of  $3 \times 10^6$ , and a maximal injection time of 80 ms in a scan range of 300–1500  $m/z$ . Precursors with a charge state of  $> 1$ , a minimum AGC target of  $1 \times 10^3$  and intensities higher than  $1 \times 10^4$  were selected for fragmentation. Peptide fragments were generated by HCD (higher-energy collisional dissociation) with a normalized collision energy of 27% and recorded in the Orbitrap at a resolution of  $R=17\,500$ . Moreover, the AGC target was set to  $1 \times 10^5$  with a maximum injection time of 100 ms. Dynamic exclusion duration was set to 60 s, and isolation was performed in the quadrupole using a window of 1.6  $m/z$ .

Peptide identification and quantification were performed using MaxQuant<sup>[73]</sup> (version 1.6.17.0). MS spectra were searched against the *Homo sapiens* UniProt Reference proteome (Swiss-Prot annotated proteins only, retrieved 27.04.21) alongside a list of common



contaminants. The search results were filtered to a 1% false discovery rate (FDR) for proteins, peptides and peptide-spectrum matches. Contaminants and proteins which were identified in <2 out of 3 probe-treated samples were removed. Protein intensity distributions were subjected to  $\log_2$  transformation and column-wise median normalization. Missing values were imputed from a normal distribution (width 0.3, down shift 1.8, total matrix). Fold change and significance of protein enrichment upon probe treatment vs. DMSO control were calculated using an empirical Bayes method for two group comparison implemented<sup>[42]</sup> with the R Bioconductor package *limma*.<sup>[43]</sup> The proteomics data have been deposited at the ProteomeXchange Consortium<sup>[74]</sup> via the PRIDE<sup>[44]</sup> partner repository with the data set identifier PXD035410.

**Labeling of recombinant legumain spiked into lysate:** HEK293 cells cultivated in a T175 culture flask were detached using Accutase, collected by centrifugation and washed three times with PBS. The cells were resuspended using 5 mL of cold lysis buffer (1% NP40 substitute, 1% sodium deoxycholate and 1×Roche cOmplete™ EDTA-free mini protease inhibitor cocktail in PBS) and lysed (4°C, 10 min) and sonicated (2×10 s pulses, 20% amplitude). The lysates were clarified (15 min, 4°C, 13000 rpm), and the protein concentration of the supernatant determined by BCA assay (Roti Quant, Roth). For each sample, 2  $\mu$ L of recombinant human prolegumain (440  $\mu$ g mL<sup>-1</sup> in 20 mM Tris, 120 mM NaCl, and 20% glycerol, pH 7.5, R&D systems, Biotechne, 2199-CY) was added to 5  $\mu$ g of lysate in a total volume of 10  $\mu$ L lysis buffer. Samples were treated for 2 h (37°C, 1000 rpm) at final concentrations of either DMSO vehicle only (2% v/v), PCB probe 16 (20  $\mu$ M), or PCB probe 17 (20  $\mu$ M) plus PCB (2 mM). The samples were then subjected to a click reaction using 0.2 mM 5-TAMRA-azide (10 mM stock in DMSO, baseclick, BCFA-008), 1 mM TCEP (52 mM stock in ddH<sub>2</sub>O, Roth), 0.1 mM TBTA ligand (1.67 mM stock in 4:1 *t*-butanol/DMSO, TCI), and 1 mM CuSO<sub>4</sub> (50 mM stock in ddH<sub>2</sub>O) for 1 h (25°C, 1000 rpm shaking). The reaction mixtures were then diluted with 10  $\mu$ L 2× SDS loading buffer (63 mM Tris·HCl, 10% glycerol, 139 mM SDS, 0.0025% bromophenol blue, 5% 2-mercaptoethanol), and the samples heated for 5 min at 95°C. Each sample was mixed and then loaded on a SDS-PAGE gel (12.5% acrylamide). A FujiFilm LAS 4000 luminescent image analyzer equipped with a Fujinon VRF43LMD3 lens and a 575DF20 filter (both FujiFilm) was used to fluorescently image the gel. Total protein content was monitored by staining with Coomassie Brilliant Blue.

**In vitro legumain activity assay:** This assay was performed according to reported procedures<sup>[75,76]</sup> with the following modifications: recombinant human prolegumain (440  $\mu$ g mL<sup>-1</sup> in 20 mM Tris, 120 mM NaCl, and 20% glycerol, pH 7.5, R&D systems, Biotechne, 2199-CY) was diluted to a 100  $\mu$ g mL<sup>-1</sup> solution with activation buffer (50 mM sodium acetate, 100 mM NaCl, 1 mM DTT, pH 4.0) and incubated for 2 h (37°C, 800 rpm) to generate the activated enzyme. The enzyme was then diluted to 0.4  $\mu$ g mL<sup>-1</sup> in assay buffer (39.5 mM citric acid, 121 mM Na<sub>2</sub>HPO<sub>4</sub>, 1 mM EDTA, 1 mM DTT, 0.1% (w/v) CHAPS, pH 5.8) and kept on ice. A concentration series of PCB (0–1.5 mM) was prepared in assay buffer with 2% (v/v) DMSO. 25  $\mu$ L of each PCB concentration and 25  $\mu$ L of activated enzyme solution were aliquoted per well in triplicate in black 96 well plates. In additional wells, no enzyme controls were used with the highest concentration of PCB. Edge wells were filled with water (50  $\mu$ L), and the plate incubated for 2 h (37°C, 200 rpm). Directly before use, a 200  $\mu$ M solution of substrate Z-Ala-Ala-Asn-AMC (Bachem, #-1865) in assay buffer was prepared from a 10 mM stock in DMSO, and then 50  $\mu$ L aliquoted to each well. The final concentrations used per well were: activated legumain 2 nM (0.1  $\mu$ g mL<sup>-1</sup>), substrate 100  $\mu$ M, PCB compound (0–375  $\mu$ M). Fluorescence ( $\lambda_{\text{ex}}=380$  nm,  $\lambda_{\text{em}}=460$  nm) was then measured (20 s kinetic cycle for 1 h) in a Tecan Infinite M Nano+ plate reader.

Initial reaction rates (RFU/s) were calculated and normalized to the DMSO only control to generate relative legumain activity values presented as percentages. The experiment was repeated 4 times.

## Acknowledgements

This work was supported by funding from the European Molecular Biology Organization [ALTF 484-2020] (I.V.L.W.), from the Deutsches Zentrum für Infektionsforschung (German Center for Infection Research, DZIF) (H. B.-O. and C. H.), from the Danish Agency for Science, Technology and Innovation [J nr.: 9-2013-1] (L. P. C.) and from the European Research Council (ERC) and the European Union's Horizon 2020 research and innovation program [grant agreement no. 725085, CHEMMINE, ERC consolidator grant] (S.A.S.). H. B.-O., L. M. and C. H. acknowledge support from the Cluster of Excellence EXC 2124: Controlling Microbes to Fight Infection (CMFI, project ID 390838134). We thank greenValley Naturprodukte GmbH for a donation of the LinaBlue used in this study, Stephan Liu for assistance with the purification of phycocyanobilins, and Andreas Vorbach for establishing the serum-free cell culture assay. Open Access funding enabled and organized by Projekt DEAL.

## Conflict of Interest

The authors declare no conflict of interests.

## Data Availability Statement

The data that support the findings of this study are available in the supplementary material of this article.

**Keywords:** antioxidants · electrophiles · legumain · natural products · proteomics · spirulina

- [1] B. Fernández-Rojas, J. Hernández-Juárez, J. Pedraza-Chaverri, *J. Funct. Foods* **2014**, *11*, 375–392.
- [2] M. R. O. B. da Silva, G. M. da Silva, A. L. F. da Silva, L. R. A. de Lima, R. P. Bezerra, D. de A. V. Marques, *ACS Chem. Biol.* **2021**, *16*, 2057–2067.
- [3] E. Manirafasha, T. Ndikubwimana, X. Zeng, Y. Lu, K. Jing, *Biochem. Eng. J.* **2016**, *109*, 282–296.
- [4] F. Pagels, A. C. Guedes, H. M. Amaro, A. Kijjoa, V. Vasconcelos, *Biotechnol. Adv.* **2019**, *37*, 422–443.
- [5] D. V. L. Sarada, C. S. Kumar, R. Rengasamy, *World J. Microbiol. Biotechnol.* **2011**, *27*, 779–783.
- [6] Q. Wu, L. Liu, A. Miron, B. Klímová, D. Wan, K. Kuča, *Arch. Toxicol.* **2016**, *90*, 1817–1840.
- [7] S. Benedetti, F. Benvenuti, S. Scoglio, F. Canestrari, *J. Med. Food* **2010**, *13*, 223–227.
- [8] A. C. Bulmer, K. Ried, J. T. Blanchfield, K. H. Wagner, *Mutat. Res. Rev. Mutat. Res.* **2008**, *658*, 28–41.
- [9] T. Hirata, M. Tanaka, M. Ooike, T. Tsunomura, M. Sakaguchi in *J. Appl. Phycol.*, Springer, **2000**, pp. 435–439.
- [10] J. Zheng, T. Inoguchi, S. Sasaki, Y. Maeda, M. F. Mccarty, M. Fujii, N. Ikeda, K. Kobayashi, N. Sonoda, R. Takayanagi, J. Zheng, T. Inoguchi, S. Sasaki, Y. Maeda, M. Mf, N. Ikeda, K. Kobayashi, N. Sonoda, T. R. Phycocyanin, *Am. J. Physiol. Regul. Integr. Comp. Physiol.* **2013**, *304*, 110–120.

- [11] M. Cervantes-Llanos, N. Lagumersindez-Denis, J. Marín-Prida, N. Pavón-Fuentes, V. Falcon-Cama, B. Piniella-Matamoros, H. Camacho-Rodríguez, J. R. Fernández-Massó, C. Valenzuela-Silva, I. Raíces-Cruz, E. Pentón-Arias, M. M. Teixeira, G. Pentón-Rol, *Life Sci.* **2018**, *194*, 130–138.
- [12] R. Koníčková, K. Vanková, J. Vaníková, K. Vánová, L. Muchová, I. Subhanová, M. Zadinová, J. Zelenka, A. Dvorák, M. Kolár, H. Strnad, *Ann. Hepatol.* **2014**, *13*, 273–283.
- [13] S. A. Basdeo, N. K. Campbell, L. M. Sullivan, B. Flood, E. M. Creagh, T. J. Mantle, J. M. Fletcher, A. Dunne, *Transl. Res.* **2016**, *178*, 81–94.
- [14] J. Marín-Prida, N. Pavón-Fuentes, A. Llópiz-Arzuaga, J. R. Fernández-Massó, L. Delgado-Roche, Y. Mendoza-Marí, S. P. Santana, A. Cruz-Ramírez, C. Valenzuela-Silva, M. Nazábal-Gálvez, A. Cintado-Benítez, G. L. Pardo-Andreu, N. Polentarutti, F. Riva, E. Pentón-Arias, G. Pentón-Rol, *Toxicol. Appl. Pharmacol.* **2013**, *272*, 49–60.
- [15] Y. Li, *J. Immunol. Res.* **2022**, *2022*, 1–8.
- [16] R. Stocker, *Antioxid. Redox Signal.* **2004**, *6*, 841–849.
- [17] D. Chen, J. D. Brown, Y. Kawasaki, J. Bommer, J. Y. Takemoto, *BMC Biotechnol.* **2012**, *12*, 1–10.
- [18] W. J. Cole, D. J. Chapman, H. W. Siegelman, *J. Am. Chem. Soc.* **1967**, *89*, 3643–3645.
- [19] B. L. Schram, H. H. Kroes, *Eur. J. Biochem.* **1971**, *19*, 581–594.
- [20] J. C. Lagarias, A. N. Glazer, H. Rapoport, *J. Am. Chem. Soc.* **1979**, *101*, 5030–5037.
- [21] A. Gossauer, *Tetrahedron* **1983**, *39*, 1933–1941.
- [22] R. W. Schoenleber, Y. Kim, H. Rapoport, *J. Am. Chem. Soc.* **1984**, *106*, 2645–2651.
- [23] J. E. Bishop, H. Rapoport, A. V. Klotz, C. F. Chan, P. Fiiglistaller, H. Zuber, *J. Am. Chem. Soc.* **1987**, *109*, 875–881.
- [24] J. E. Bishop, J. Nagy, J. F. O. Connell, H. Rapport, *J. Am. Chem. Soc.* **1991**, *113*, 8024–8035.
- [25] B. E. Fu, L. Friedman, H. W. Siegelman, E. Fu, L. Friedman, H. W. Siegelman, *Biochem. J.* **1979**, *179*, 1–6.
- [26] R. J. Beuhler, R. C. Pierce, L. Friedman, H. W. Siegelman, *J. Biol. Chem.* **1976**, *251*, 2405–2411.
- [27] C. C. Moraes, L. Sala, G. P. Cerveira, S. J. Kalil, *Braz. J. Chem. Eng.* **2011**, *28*, 45–49.
- [28] M. C. Roda-Serrat, K. V. Christensen, R. B. El-Houri, X. Fretté, L. P. Christensen, *Food Chem.* **2018**, *240*, 655–661.
- [29] T. Kamo, T. Eki, Y. Hirose, *Plant Cell Physiol.* **2021**, *62*, 334–347.
- [30] S. L. Minic, M. Milcic, D. Stanic-Vucinic, M. Radibratovic, T. G. Sotirioudis, M. R. Nikolic, T. C. Velickovic, *RSC Adv.* **2015**, *5*, 61787–61798.
- [31] G. Castro-Falcon, D. Hahn, D. Reimer, C. C. Hughes, *ACS Chem. Biol.* **2016**, *11*, 2328–2336.
- [32] A. Jenmalm-Jensen, I. Cornella Taracido in *Target Discovery and Validation: Methods and Strategies for Drug Discovery*, Vol. 78 (Ed.: A. T. Plowright), Wiley, Weinheim, **2019**, pp. 25–49.
- [33] T. Werner, M. Steidel, H. C. Eberl, M. Bantscheff in *Quantitative Methods in Proteomics. Methods in Molecular Biology*, Vol. 2228 (Eds.: K. Marcus, M. Eisenacher, B. Sitek), Humana, New York, **2021**, pp. 237–252.
- [34] B. F. Cravatt, A. T. Wright, J. W. Kozarich, *Annu. Rev. Biochem.* **2008**, *77*, 383–414.
- [35] K. Kubota, M. Funabashi, Y. Ogura, *Biochim. Biophys. Acta Proteins Proteomics* **2019**, *1867*, 22–27.
- [36] M. H. Wright, S. A. Sieber, *Nat. Prod. Rep.* **2016**, *33*, 1–28.
- [37] I. V. L. Wilkinson, G. C. Terstappen, A. J. Russell, *Drug Discovery Today* **2020**, *25*, 1998–2005.
- [38] S. H. L. Verhelst, M. Bogyo, *BioTechniques* **2005**, *38*, 175–177.
- [39] C. G. Parker, M. R. Pratt, *Cell* **2020**, *180*, 605–632.
- [40] E. Smith, I. Collins, *Future Med. Chem.* **2015**, *7*, 159–183.
- [41] S. Minic, D. Stanic-Vucinic, M. Radomirovic, M. Radibratovic, M. Milcic, M. Nikolic, T. Cirkovic Velickovic, *Food Chem.* **2018**, *239*, 1090–1099.
- [42] W. Aftab, *LIMMA proteomics pipeline*, DOI: 10.5281/zenodo.3727202, n.d.
- [43] M. E. Ritchie, B. Phipson, D. Wu, Y. Hu, C. W. Law, W. Shi, G. K. Smyth, *Nucleic Acids Res.* **2015**, *43*, e47.
- [44] Y. Perez-Riverol, A. Csordas, J. Bai, M. Bernal-Llinares, S. Hewapathirana, D. J. Kundu, A. Inuganti, J. Griss, G. Mayer, M. Eisenacher, E. Pérez, J. Uszkoreit, J. Pfeuffer, T. Sachsenberg, Ş. Yilmaz, S. Tiwary, J. Cox, E. Audain, M. Walzer, A. F. Jarnuczak, T. Ternent, A. Brazma, J. A. Vizcaino, *Nucleic Acids Res.* **2019**, *47*, D442–D450.
- [45] K. Kammers, R. N. Cole, C. Tiengwe, I. Ruczinski, *EuPA Open Proteomics* **2015**, *7*, 11–19.
- [46] E. Dall, H. Brandstetter, *Proc. Natl. Acad. Sci. USA* **2013**, *110*, 10940–10945.
- [47] E. Dall, V. Stanojlovic, F. Demir, P. Briza, S. O. Dahms, P. F. Huesgen, C. Cabrele, H. Brandstetter, *ACS Catal.* **2021**, *11*, 11885–11896.
- [48] N. Matarasso, S. Schuster, A. Avni, *Plant Cell* **2005**, *17*, 1205–1216.
- [49] E. Dall, H. Brandstetter, *Biochimie* **2016**, *122*, 126–150.
- [50] E. Dall, H. Brandstetter, *Acta Crystallogr. Sect. F* **2012**, *68*, 24–31.
- [51] B. Manoury, E. W. Hewitt, N. Morrice, P. M. Dando, A. J. Barret, C. Watts, *Nature* **1998**, *396*, 695–699.
- [52] R. Maehr, H. C. Hang, J. D. Mintern, Y.-M. Kim, A. Cuvillier, M. Nishimura, K. Yamada, K. Shirahama-Noda, I. Hara-Nishimura, H. L. Ploegh, *J. Immunol.* **2005**, *174*, 7066–7074.
- [53] F. E. Sepulveda, S. Maschalidi, R. Colisson, L. Heslop, C. Ghirelli, E. Sakka, A. M. Lennon-Duménil, S. Amigorena, L. Cabanie, B. Manoury, *Immunity* **2009**, *31*, 737–748.
- [54] S. Maschalidi, S. Hässler, F. Blanc, F. E. Sepulveda, M. Tohme, M. Chignard, P. van Endert, M. Si-Tahar, D. Descamps, B. Manoury, *PLoS Pathog.* **2012**, *8*, e1002841.
- [55] B. D. Reddy, N. M. Beeraka, C. M. K. Chitturi, S. V. Madhunapantula, *Curr. Pharm. Des.* **2020**, *27*, 3337–3348.
- [56] C. Liu, C. Sun, H. Huang, K. Janda, T. Edgington, *Cancer Res.* **2003**, *63*, 2957–2964.
- [57] N. Li, Q. Liu, Q. Su, C. Wei, B. Lan, J. Wang, G. Bao, F. Yan, Y. Yu, B. Peng, J. Qiu, X. Yan, S. Zhang, F. Guo, *Med. Oncol.* **2013**, *30*, 621.
- [58] P. Guo, Z. Zhu, Z. Sun, Z. Wang, X. Zheng, H. Xu, *PLoS One* **2013**, *8*, e73090.
- [59] Y. Zhen, G. Chunlei, S. Wenzhi, Z. Shuangtao, L. Na, W. Rongrong, L. Xiaohe, N. Haiying, L. Dehong, J. Shan, T. Xiaoyue, X. Rong, *Sci. Rep.* **2015**, *5*, 16599.
- [60] W. Zhang, Y. Lin, *Cells* **2021**, *10*, DOI: 10.3390/cells10051153.
- [61] A. A. Kembhavi, D. J. Buttle, C. G. Knight, A. J. Barrett, *Arch. Biochem. Biophys.* **1993**, *303*, 208–213.
- [62] G. S. Jensen, C. Drapeau, M. Lenninger, K. F. Benson, *J. Med. Food* **2016**, *19*, 645–653.
- [63] M. Poreba, R. Solberg, W. Rut, N. N. Lunde, P. Kasperkiewicz, S. J. Snipas, M. Mihelic, D. Turk, B. Turk, G. S. Salvesen, M. Drag, *Cell Chem. Biol.* **2016**, *23*, 1023–1035.
- [64] K. A. Ness, S. L. Eddie, S. Burton, T. Harrison, P. Mullan, R. Williams, *Bioorg. Med. Chem. Lett.* **2016**, *26*, 413–416.
- [65] J. Lee, M. Bogyo, *Bioorg. Med. Chem. Lett.* **2012**, *22*, 1340–1343.
- [66] A. Ovat, F. Muindi, C. Fagan, M. Brouner, E. Hansell, J. Dvořák, D. Sojka, P. Kopáček, J. H. McKerrow, C. R. Caffrey, J. C. Powers, *J. Med. Chem.* **2009**, *52*, 7192–7210.
- [67] K. Loak, D. N. Li, B. Manoury, J. Billson, F. Morton, E. Hewitt, C. Watts, *Biol. Chem.* **2003**, *384*, 1239–1246.
- [68] A. J. Niestroj, K. Feußner, U. Heiser, P. M. Dando, A. Barrett, B. Gerhartz, H. U. Demuth, *Biol. Chem.* **2002**, *383*, 1205–1214.
- [69] K. A. Ness, S. L. Eddie, C. A. Higgins, A. Templeman, Z. D'Costa, K. K. D. Gaddale, S. Bouzzaoui, L. Jordan, D. Janssen, T. Harrison, F. Burkamp, A. Young, R. Burden, C. J. Scott, P. B. Mullan, R. Williams, *Bioorg. Med. Chem. Lett.* **2015**, *25*, 5642–5645.
- [70] M. Poreba, *Biol. Chem.* **2019**, *400*, 1529–1550.
- [71] J. B. Patel, F. R. Cockerill, P. A. Bradford, G. M. Eliopoulos, J. A. Hindler, S. G. Jenkins, J. S. Lewis, B. Limbago, L. A. Miller, D. P. Nicolau, M. Powell, J. M. Swenson, J. D. Turnidge, M. P. Weinstein, B. L. Zimmer. 2015. Methods for dilution antimicrobial susceptibility tests for bacteria that grow aerobically. Approved Standard – Tenth Edition, vol 35. Clinical and Laboratory Standards Institute, USA.
- [72] L. Maier, M. Pruteanu, M. Kuhn, G. Zeller, A. Telzerow, E. E. Anderson, A. R. Brochado, K. C. Fernandez, H. Dose, H. Mori, K. R. Patil, P. Bork, A. Typas, *Nat. Publ. Gr.* **2018**, *555*, 623–628.
- [73] J. Cox, M. Mann, *Nat. Biotechnol.* **2008**, *26*, 1367–1372.
- [74] J. A. Vizcaino, E. W. Deutsch, R. Wang, A. Csordas, F. Reisinger, D. Rios, J. A. Dienes, Z. Sun, T. Farrar, N. Bandeira, P. A. Binz, I. Xenarios, M. Eisenacher, G. Mayer, L. Gatto, A. Campos, R. J. Chalkley, H. J. Kraus, J. P. Albar, S. Martinez-Bartolomé, R. Apweiler, G. S. Omenn, L. Martens, A. R. Jones, H. Hermjakob, *Nat. Biotechnol.* **2014**, *32*, 223–226.
- [75] T. J. Perlenfein, J. D. Mehlhoff, R. M. Murphy, *J. Biol. Chem.* **2017**, *292*, 11485–11498.
- [76] R. Solberg, R. Smith, M. Almlöf, E. Tewolde, H. Nilsen, H. T. Johansen, *Biol. Chem.* **2015**, *396*, 71–80.

Manuscript received: August 8, 2022  
Revised manuscript received: December 19, 2022  
Accepted manuscript online: December 20, 2022  
Version of record online: January 26, 2023